The distant tail behavior during high speed solar wind streams and magnetic storms

C. M. Ho and B. T. Tsurutani
Jet Propulsion Laboratory, California Institute of Technology, Pasadena, CA 91109

Abstract. We have examined the ISEE-3 distant tail data during three intense (Dst < -100 nT) magnetic storms and have identified the tail response to high speed solar wind streams, interplanetary magnetic clouds, and near-earh storms. The three storms have a peak Dst ranging from -150 to -220 nT, and occur on Jan. 9, Feb. 4 and Aug. 8, 1983. During the storm onsets, the fast solar wind and magnetic field dynamic pressure ($B^2/8\pi+\sum n_i kT_i$) fluctuations moved the tail across the spacecraft multiple times. Tbc magnetotail is strongly compressed by the outside sheath pressure. The lobe field strength can usually be predicted by the pressure balance. The strongest lobe field magnitude detected is 37 nT during storm main phase on Jan. 10, which is higher than the sheath field by 5 - 10 nT. The sheath plasma pressure accounts for the higher lobe field strengths. However, for the Feb. 4 storm, wc find that 3 tail lobe encounters are not in static balance with sheath pressure. During the storm times, the. field magnitudes of the lobe and plasmasheet increase by a factor of 3-5 relative to the quiet time. The temperature anti density in both regions aiso increase by factors of 2-3, but with little plasma β changes, as one would expect. Under the assumption of tail flux conservation, increased sheath pressure implies a reduced tail sire. Besides the tail size changes, the location of the nominal tail axis is controlled by solar wind flow orientation. This study shows that more than 70% of tail in-and-out events are predicted by either of these external mechanisms (changes of tail size due to the external pressure and the solar wind directional changes). Nine tail plasmasheet jettings and Twelve slow-mode shocks have been detected during the three storms. One remarkable feature of the jettings is very strong earthward flow (up to 1200 km/s) and tailward flow (up to 1500 km/s). 'l'he solar wind speed for these events was only -900 km/s. Both tail fiow events have the highest speeds found to date. The preponderance of such a strong earthward flow indicates that during magnetic storms, magnetic reconnection occurs at locations well beyond the distance of ISEE-3. Through the interface of slow-mode shocks between the tail lobe and the plasmasheet/boundary layer, magnetic energy is being converted into plasma thermal and kinetic energy by the magnetic merging process. The predicted downstream plasma jetting speed (978 km/s) is consistent with the observations (1 000 km/s) in the boundary layer. One surprising feature is that this reconnection process seems to be quite prominent during the storm recovery phase. One possible suggestion is that the dynamics of the distant taii are not at all related to magnetic storms and substorms, but is an after-effect, releasing extra magnetic tail energy by field sloughing via these reconnection events, accompanying the plasmasheet expansion.

1. Introduction

How the interplanetary parameters control the distant tail behavior is still not very well understood. *Fairfield* [1993] suggests tha[a long duration northward interplanetary magnetic field (IMF) can result in a disappearance of the distant tail. Using ISEE-3 data, statistical studies from *Tsurutani et al.* [1986] show that the taii lobe field strength is well correlated with the geomagnetic activity indices Kp anti AE. The lobe field strength generally increases with increasing geomagnetic activity. Why such changes occur in the distant tail arc not well understood. It is well known that if the IMF has a southward component, major magnetic flux erosion at the magnetopause will occur, with greater tail flaring anti consequently greater tail compression as suggested by *Coroniti and Kennel* [1972]. Based on a flaring-tail model, *Tsurutani et al.* [1986] find that with erosion at the magnetopause and a large solar wind ram pressure, the flaring termination may reach a distance beyond 240 R_e. The tail field strength substantially increases inside iOO R_e, but essentially negligible changes at large distance > 140 R_e. Thus, increases in the distant tail field strength as a function of Kp anti AE may be due to other reasons rather than near-earth magnetic merging.

Using recent GEOTAIL data, the distant tail dynamics during magnetic storms, solar wind flow, and IMF variations have measurement part of the instrument was not functional during the ISEE-3 distant tail passes.

3. observations

3.1 Tail Magnetic Field and Plasma Characteristics: From the examination of all distant tail measurements taken during the three storms, many large spike-like variations in the velocity, plasma density and temperature can be noted (not shown). These variations are indicative of multi-tail lobe, plasmasheet and sheath encounters (this will be demonstrated later). Thus the. data is a combination of observations in the magnetosheath, tail lobe and plasmasheet. However, a clear trend can be seen in the magnetic field and velocity magnitudes during, the storm main phase. 'l'his will help in the identification of the various regions within which the spacecraft is located. Wc thus first need to formulate criteria to identify each region in detail before we can proceed to characterize the properties of various tail regions during the storms.

Based on previous studies [*Zwickl et al.*, 1985; *Slavin et al.*, 1985] and our recent/past experience [*Ho et al.*, 1994; 1996], the lobes, plasmasheet and sheath during quiet or substorm times arc identified to have the following, characteristics. The tail lobes have stable magnetic fields (mainly in the B_x component, > 8 nT), lower plasma velocities (usually less than 200 km/s), the lowest plasma densities (< 0.2 cm^{-3}) , intermediate temperatures (higher than the sheath, but lower than the plasmasheet: 1.2 x $10^6 > T_e > 6.5 \times 10^5$ K). The plasmasheet region is usually characterized by the lowest (< 2 nT) and most turbulent magnetic fields, B_x reversal, the highest temperatures ($T_e > 1.2 \times 10^6$K), densities in the range from 0.2 to 1.0 cm-?', anti high plasma velocities (> 500 km/s). In contrast, the. magnetosheath usually has cold temperatures ('1', < 6.5x 10^5K), high densities ($n_e > 1.0$ cm^{-3}), turbulent fields, and a relatively constant solar wind speed (- 400 km/s). Using these criteria, we will examine data from all three storms, Because the second storm includes two main phases and is more complicated, wc will study this event last. '1'bus, wc will study the three storms in an order of events 1, 3 and 2.

Figure 2 gives ISEE-3 distant tail observations for the first magnetic storm (Jan. 9, 1983). From top to bottom arc the AE and Dst indices, the three magnetic field components, field magnitude, two plasma velocity components, velocity magnitude, electron density, and temperature. During [his storm, ISEE-3 was 33 R_e away from the nominal tail axis (near the tail boundary), but only 2-4 R_e from the X-Y plane. ISEE-3 is in the magnetosheath for most of the time. At - 1600 UT, day 9, there is an interplanetary shock leading a solar ejecta event. The shock (S) is identified by the abrupt jump in magnetic field magnitude from -6 to ~16 nT, velocity from -400 to 600 km/s, density from 8 to 25 cm^{-3}, and temperature from -2x 10^5 to -3x10^5K. The IMF B_z is relatively steady, at a value near O nT, so the Dst response is only slight. There is a small southward component just behind the shock that causes a -1300" nT (AE) substorm.

A large southward turning in the field occurs at -0140 UT, day 10. This turning causes a substorm onset (SO) with ~1200 nT in AE. The B_z configuration is southward then northward spanning an interval to -0400 UT, day 11. The magnetic field is smooth and relatively free of waves and discontinuities. We identify this as the driver gas of the solar ejecta [*Tsurutani et al.*, 1988] and tbc south-north rotation, a magnetic cloud [*Klein and Burlaga*, 1982]. The southward turning of the sheath field creates the main phase (Ml') of the magnetic storm. The northward turning at -0900 UT clay 10 leads to the start of the recovery phase (R P). The interplanetary interval from the shock to the driver gas creates the storm initial phase (11'). Wc have marked these intervals using vertical lines and letter abbreviations in the figure.

During the initial phase, two tail lobe encounters arc. detected, which have large B_x and |B| > 20 nT. The magnetic storm (Dst --220 nT) is triggered by a stable and very large southward B_z (~-25 nT). During the recover phase wc see a strong negative B_y (-25 - -30 nT). At about 0900 UT, there is a tail lobe encounter which has the largest magnetic field (37 nT) magnitude wc found, about 10 nT higher than the sheath field, During the tail encounter, the plasma flow speed drops to < 200 km/s. The magnetic field shows very small B_y and B_z components. We do not scc any plasma jetting events during this particular storm.

During the third magnetic storm (Aug. 7, 1983), ISEE-3 is located about -220 R_e in the distant tail. The distance from the nominal tail axis is between 12 and 14 R_e (inside the tail). All ISEE-3 observations arc. shown in Figure 3 with [he same format as Figure 2. At 2100 UT, the solar wind speed jumps from 400 to 500 km/s. No obvious interplanetary shock and storm initial phase arc identified, The storm main phase starts at 2150 UT', when the magnetic field first turns southward accompanied by a large negative B_y (--25 nT). The earliest tail encounter (northern tail lobe - 20 nT) is found at 2115 UT, only 10 min after a substorm onset. At 2240 UT, there is another transient southern tail lobe crossing. The field strength was 33 nT, which is higher than the sheath field by 2 - 7 nT. The solar wind plasma pressure must account for tbc missing tail pressure, At -0100 UT, Aug. 8, B_z turns deeply southward again and B_y has also a reversal. At -0700 UT, Dst reaches its maximum by 150 nT, and then a recovery phase starts immediately after B_z returns to -O nT. Other tail crossings are detected at around 0800 UT. 'I'he plasma bulk velocity usually drops to small values (< 200 km/s) for these tail encounters. During this storm, wc scc two earthward plasma jettings with a speed of about + 500 km/s. After 1400" UT, Aug. 9, the spacecraft mainly stays inside the tail lobe and plasmasheet. We. see many bidirectional (+500 to -800 km/s) plasma flow events.

Compared to the first and third storms, the second storm event lasts much longer and has more tail crossings. Eight days of distant tail observations during the storm arc shown in Figure 4 with the same. format as before, An interplanetary shock occurs at 1700 UT, Feb. 4, 1983. Around the shock the.re is a brief initial phase and a sudden impulse (S1). The southward field fluctuations after the shock trigger the storm main phase and substorm onset, However, closer inspection indicates that this storm consists of two main phases (MPa and MPb) and two recovery phases (RPa and RPb). Dst suddenly decrease s to -170 nT in the first main phase and then quickly recovers (RPa). When Dst returns to -100 nT, A large B_z southward turning causes the second main phase and another substorm onset at 0200 UT of day 36. Even though this occurs exactly 26 days after the first magnetic storm, the high speed (- 900 km/s) solar wind stream and magnetic field have different features from the first storm on day 10. During the second main phase (MPb) of the storm, Dst decreases again to reach its minimum -185 nT. This storm then gradually recovers (RPb) to the normal values until day 42. Daring, this recovering process, wc can scc many substorm events due to B_z southward fluctuations, The AE index has many peaks ranging from 500 to 2000 nT. Because there are so many tail encounters during this storm, these regions are not easily identified as in previous two storms. We need to osc the criteria wc developed to examine two days of storm data in high time resolution.

Figure 5a shows a 12 hour interval of data prior to the storm on Feb. 4, 1983 during interplanetary quiet. At the top of the figure is our legend. We have used a blank box to represent the magnetosheath region, hatched hox for the tail lobe, and black box for plasmasheet/boundary layer. During the 12 hours, AE is below 400 nT. The spacecraft is in.side the tail most of time. The fields (B_x and B) are very stable (mostly in south lobe, --10 nT). The plasma speed inside the tail is below 200 km/s. in contrast, in the magnetosheath the magnetic field is low (< 8 nT), and solar wind velocity is also stable. at 400 km/s. The sheath plasma density is large (> 1 cm^{-3}). During such quiet intervals wc expect a clear pressure balance between the tail lobe and magnetosheath. The spacecraft occasionally crosses the plasmasheet, where there arc high plasma temperatures and low fields. These arc easily identifiable. During this period, ISEE-3 is about 11 R_e away from the nominal tail axis (aberration corrected).

Figure 5b gives the second 12 hours of data including the first main phase (MPa) of storm 2. At 1610 U']', an interplanetary shock occurs. At the same time, a sudden impulse is detected at ground stations, This impulse causes the storm and substorm onsets. Then the spacecraft is in the sheath, The velocity, density and magnetic field all suddenly increase, The field B_z component has a southward turning and then a large fluctuation ($\pm$ 15 nT) is followed. 'E'he shocked plasma temperature increases from 2x 10s to $6x10^5$K. 'l'he density increases from 5 to -60 cm^{-3}. The magnetic field magnitude jumps from 16 nT to ~48 nT. The tailward plasma speed, V_{tw} (-V,), also jumps to --1000 km/s. At 1640 UT around the shock, there is a S minute interval with very high temperature (2.0x 10^6K) and low density. This region probably is a lobe crossing (also probably a plasmasheet crossing). After a data gap of 1730-2000 UT, we see that the spacecraft continuously stays inside the sheath, But the storm quickly recovers because B_z becomes more northward.

In Figure SC, wc show the third 12 hours of data with the second main phase (MPb) of storm 2. The large interplanetary magnetic field with large + B_z and -B_y components has a sudden southward B_z turning (from +25 to -23 nT) at 0200 UT of day 36. Then the stable southward IMF and MPb last at least 8 hours. The sheath high speed stream has a constant tailward Speed of - 1000 km/s. At 0235 UT the first tail lobe crossing after the storm onset is detected. Wc see a large B_x, high temperature, and reduced velocity and density during this lobe crossing The interesting finding is that for this crossing the lobe field magnitude is significantly lower (by 13 n']") than outside the sheath. Even though the lobe field has a large B_x, its B_y and B_z components arc much less than those inside the magnetosheath. We also find that two other lobe crossings occurring at 0410 UT and 0430 UT have lower fields than the adjacent sheath fields. The plasma density inside the lobe is 5-10 times lower than outside sheath, while temperature is only 2-3 times higher than outside. Thus, [his phenomenon is different from what we seen from storms 1 and 3. The difference suggests that temporally there is a total pressure unbalance between the sheath and the. tail lobe. The high density plasma and strong field will continue to squeeze the tail until finally they both reach a balance. After 0430 UT, the tail lobe encounters show the lobe field magnitude higher than the sheath field, because IMF B_y and B_z components inside the sheath have significantly decreased. Thus the pressures on both sides arc balanced.

Wc scc more plasma jetting and slow shock events in the last 12 hours shown in Figure 5d. Between 1930 and 2000 UT, the. earthward jetting has a speed as high as 1000 km/s. These jetting events arc seen in the plasmasheet and lobe/boundary layer regions. Large tailward jettings with speeds greater than 1500 km/s arc detected at 0630 and 1520 UT. These jettings show that reconnection processes arc taking place in the distant tail. We will discuss these plasma jetting and slow shock events later.

Wc summarize all characteristics for three distant regions during both storm anti quite times in "1'able 2. These values arc obtained by averaging the field and plasma parameters. '1'here arc 74 tail lobe encounters (54 during the storms), 9 plasma jetting events and 12 slow-mode shocks from three storms. Wc find that during storms, the field magnitudes of the lobe and plasmasheet increase by a factor of 3-5 relative to the quiet time. The temperature anti density in both regions also increases by a factor of 2-3. I'bus, there is an obvious increase in magnetic field intensity, plasma density, and temperature during storm times, as identified in previous studies [*Tsurutani et al.*, 1986]. However, the plasma β changes very little. The changes arc closely related to changes in the field and plasma in the magnetosheath.

We also examine the correlation between the AE index and all tail lobe encounters, plasma jetting events and slow-mode shocks, We find that there is a clear positive correlation between the lobe field magnitude and the AE index. However, the correlation between the earthward plasma jetting speeds in the plasmasheet and the AE index is not obvious. We see large jetting speed during both high and low AE intervals, Wc also examine the substorm dependence of the occurrence rates for these events. We use 10 rain resolution AE index for this study. All events of lobe crossings and plasma jettings inside the plasmasheet are identified to be present or not in each 10-rnin interval. Their occurrence rates are normalized by the total interval numbers, The statistical results are shown in Figure 6. From the top panel, wc scc that there arc relatively more tail lobe crossings when the AE index is between 300 and 500 nT. This is mainly attributed to spacecraft's staying inside the tail lobe during late recovery phases of storms 2 and 3. These events are detected in all AE intervals rrnd all storm phases. 14 tail lobe encounters occur in the storm main phase, while 40 appear during the recover phase. In the bottom panel, wc sec that the occurrence of the earthward jettings detected in the plasmasheet has no dependence on substorm activity. We have also used different lag times of AE inde x relative to the distant tail observations (from 20 min to 40 rein). But no obvious change is seen for their occurrence rates. Plasma jettings are seen mainly (8 events) in the early recovery phase, while one in the main phase. Out of all 9 jetting events, while 7 correspond to substorms, 2 occur during lower AE (< 200 nT). But the maximum lobe field strength detected seems to be related to the Dst (storm severity) magnitude, while jetting events secm to mainly occur during the storm recovery phase,

3.2 *Tail Pressure Balance and Solar Wind Aberration Effect:* In order to explain how the high speed solar stream and magnetic storm affect the distant tail and why there arc many tail/magnetosheath crossings during storm times, we need to examine both the changes of tail size and tail flapping. For the former, we assume pressore balance between the sheath and tail lobe. Furthermore, if we assume tail magnetic flux conservation, the increasing tail field strength will result in a smaller tail, Thus when the sheath pressure increases. as a consequence, the spacecraft which would be originally within the tail may get inro the sheath region, clue to the tail compression Secondly, in addition to an aberration angle doe to earth's motion relative to the solar wind V_x, the distant tail is also deflected due to variations of the solar wind speed V_y component (it is also possible that significant V_z variations deflect the tail, but this data is not available). Thus the tail axis will be strongly affected by both solar wind speed V_x and V_y. IMF B_y can twist the shape of tail, but cannot significantly change the location of the tail. Tail flapping can explain those transit crossings between the tail and magnetosheath, but cannot explain the long intervals (several boars) within the tail or the sheath.

We first calculate the pressure balance between the sheath anti the tail lobe during a high speed stream. Whe n the Spacecraft is inside the magnetosheath, wc may assume that the high sheath pressure squeezes the tail into a smaller region. During this time, for a steady state case, the outside sheath pressure will balance the inside tail lobe pressore. Neglecting the thermal pressure inside the tail (which is relatively small), we have:

$$\frac{B_{lobe}^2}{8\pi} = \frac{B_{sheath}^2}{8\pi} + nkT \qquad (1)$$

Thus we may predict the lobe field magnitude from direct measurements "of the magnetic field and plasma in the magnetosheath. Furthermore, wc assume the conservation of the lobe magnetic field flux, that is:

$$B_{lobe} R_{lobe}^2 = const. \qquad (2)$$

We used the previous statistical values [*Tsurutani et al.*, 1984; *Slavin et al.*, 1985] to determine the constant (when the lobe field has a magnitude of 11 nT, the tail has an average radius of 30 R_e). Using the two equations wc may calculate the lobe field and the. corresponding tail size when the spacecraft is inside the sheath region. The calculated results for the three storms arc shown in Figure 7. In the top panels of each of the three plots a, h and c, wc plot the measured magnetic field (solid line) which includes both sheath and tail regions (wrc. have shown the tail lobe encounters using shading), The dashed line is the predicted lobe field magnitude. We can see that the predicted lobe magnetic field is always larger than the sheath field, but has a comparable strength with the measured lobe field. The magnetosheath field strengths have a broad range from 5 to 60 nT. The dashed lines arc significantly higher than the sheath field, The difference is mainly due to larger sheath thermal (large plasma density) pressure,

The radius (or size) of the tail lobe based on the predicted lobe field arc plotted in a dashed line in each lower panel in Figure 7. A smaller tail radius is clearly associated with a larger lobe field and larger sheath pressure, and vice versa. The tail sizes may vary from 12 R_e to 40 R_e while the predicted lobe field varies from - SO nT in the peak of the compressed field region to 6 nT after this region, We see a gradual increase in the tail size accompanying this compressed region passover. The sizes after storms can even expand to larger than before the storms. For a reference, using a dotted line, we also plot the distance of the spacecraft from a tail axis which is only corrected by a fixed aberration (4°) angle. Finally, wc calculate a more accurate solar wind aberration angle, using measured velocities, We have used a solid line to plot the distance between the spacecraft and the corrected tail axis. When we calculate this distance, wc usc the solar wind speed V_x and V_y components measured only inside the magnetosheath. We see large variations of the distance from the corrected tail axis, doc to large. variations of solar wind velocity V_x anti V_y. Using the relative variations between the dashed and solid lines, wc can determine the spacecraft's position in the sheath or tail lobe. We can also compare this result with the location identified by the observations,

The solid line going up and down relative to the dashed line suggests the spacecraft moving into and out of the tail lobe. We sec that, for most of the time when tail lobe encounters occur, the solid lines arc below or close to the dashed lines. 'l'his shows that the spacecraft gets into the tail or detects the tail boundary, Overall, we find that the calculated locations arc consistent with the observations 70% of the time. It suggests that the tail boundary location is controlled by both the sheath pressure and solar wind flow. However, we also find that the difference between the lines is large at some times (e.g. 1200-1600, day 009; 1300-2400 UT, day 010; 2000 UT of day 036-0200 of day 037; and 2000 UT of day 219-0100 of day 220). Jn the first three intervals, the calculations show that spacecraft should be inside the tail because its distance from the tail axis is less than the tail lobe radius, while the last onc should be in the sheath. But the observations show opposite situations. 'J"his inconsistency may be caused by the variations of the solar wind speed V_z component (unfortunately, no measurements for this component arc available), unstable tail magnetic flux (lack of flux conservation) during distant reconnection or a disappearing tail during a long interval of northward IMF (for the first two intervals). We note that the plasma jetting events arc seen in the plasmasheet during two of the four intervals. It suggests that tail magnetic flux may not be a constant during the reconnection process in the distant tail, The size of the tail will not change as wc assumed during this time interval.

3.3 Plasma Jetting. $ and Slow -mode Shocks: During magnetic storms, some plasmasheet jetting and slow shock events arc detected. This suggests that the distant neutral line or magnetic merging may exist beyond the 200 R_e distant tail, We do not scc any jetting events at the first storm (Jan, 10, 1983, spacecraft location seen in Figure 1), because very few tail encounters arc seen during this storm, We see the jetting events in the other two storms, These jettings mainly appear during both storm main phases and recovery phases (when the spacecraft gets into the plasmasheet after 2000 UT of day 221 and 1200 UT of day 037, wc see frequent plasma jettings). Most of these crossings between the tail lobe and the plasmasheet boundary layer/plasmasheet have been identified as slow shocks. Thus tail lobe magnetic energy has been converted into plasma kinetic and thermal energy in the plasmasheet through the interface of the. slow-mode shock.

The highest earthward plasma jetting speed is -1200 km/s, which is detected at 0253 U'I', day 037. This is also the highest speed of earthward plasma jettings ever found in the distant tail (upstream data not available). The second highest event (V_x = 1050 km/s) is seen at 1935 U'I', day 036. Roth earthward jetting events arc detected in the recovery phase (RPb) of the second storm. in addition, some high speed tailward jettings (V_x<-1 500 km/s) also are detected. They arc much larger than the magnetosheath flow speed (-900 - 1000 km/s). These events arc the highest speeds wc found to elate,

The second highest earthward jetting event with high resolution magnetic field data has been shown in Figure 8 in a GSE frame and rotated in a shock frame, respectively. By identifying each region, we see that the earthward flow mainly appears in the plasmasheet boundary layer region (in the lobe side), instead of the plasmasheet region. Before 1925 UT, the spacecraft is inside the sheath as we identified in Figure 5d. Then the spacecraft progressively crosses the south tail lobe, boundary layer (at 1945 UT), and plasmasheet (2000 UT), and then returns to the south lobe again at 200S UT. In the GEOTAIL study of *Saito et al. [1995]*, they also find some earthward plasma flows in the lobe-like regions, Wc do not know whether or not these flows arc due to leakage of plasma from the plasmasheet to the lobe. we have used ttre coplanarity relation [e. g., *Colburn and Sonett,* 1966] to calculate the shock normal. All measured parameters arc listed in "I'able 3. 'I'hey include the upstream average magnetic field B_u, downstream field B_d, and N_e, T_e, and V for both the upstream and downstream regions, In this shock reference system, "downstream" is the boundary layer with high speed earthward flow and plasmasheet bounded by the first pair of vertical lines, and "upstream" is the tail lobe bounded by the second pair of vertical lines. Both the upstream and downstream magnetic fields arc rotated into a shock normal coordinate system. Along the shock normal, there is a significant B component (B_n = -5.23± 1.21 al') across the shock. The maximum errors in the magnetic field arc derived from the standard deviations of the upstream and downstream field values.

Wc have defined some magnetic field angles in the following to compare with the *Petschek* [1964] model. Wc have sketched the geometry of the magnetic neutral line and earthward slow shock in Figure 9. At first, wc project the magnetic field and the shock normal into the x-z plane, '1'here is a angle θ_{nz} between the normal n and the. z axis, where $\theta_{nz} = \cos^{-1} n_z$. The second angle is ξ between the shock normal in the x-z plane and the z axis, where $\xi = \tan^{-1} n_x/n_z$. The third angle is η, between the shock normal n in the x-z plane. and the field B in the x-z plane, that is, $\eta = \cos^{-1} (\mathbf{B}_{xz} \cdot \mathbf{n}_{xz} / |\mathbf{B}_{xz}||\mathbf{n}_{xz}|)$. The fourth angle χ, lies between the magnetic field line in the x-z plane and the x axis, The angle χ is the acute angle of $\eta - \xi$. We next usc the Rankine-Hugoniot conservation relations to calculate the plasma flow velocity along the normal direction in the upstream region under the assumption of the conservation of B_n, mass, tangential electric field and momentum [*Ho et al.*, 1996]. All calculated angles and speeds arc shown in I'able 3. For this case, the plasma flow velocity along the normal, V_{un} *is* greater than the slow-mode speed V_{sl} and less than the Alfven speed in the, normal V_{An}, as expected for a slow mode shock.

Then, based on the theory of *Hill* [1975] and *Vasyliunas* [1975], the outgoing plasma jetting speed in the plasmasheet, V_{xd} is

$$V_{xd} = V_{Au} \cos \chi = V_{Au} \sin(\eta - \xi) \qquad (3)$$

Using the Alfven velocities VA_u and angles listed in Table 3, we obtain an earthward plasmasheet V_{xd} of 987±45 km/s for this shock. This speed calculated from the theoretical model is consistent with the measured jetting speed (1002 km/s). Thus, this confirms the existence of a Petschek type of neutral line. High speed jetting flow is the result of reconnection in the distant tail. This result is also consistent with boundary layer plasma jettings in the picture of *Cowley et al.* [1984].

4. Discussion

In this section, we will compare our results with previous studies and discuss possible explanations for these results. *Kokubun et al.* [1996] find that most large tail events seen by GEOTAIL occur during main phases of storms. We also see these large tail field events in main phases of storms, We think that this is because high speed solar wind streams and magnetic clouds (large external pressure) occur in these phases of storms. The increase of field strength inside the tail is mainly related to an increase in outside sheath pressure, not the near-earth geomagnetic activity, We also note that enhanced sheath thermal pressure is always accompanied by enhanced dynamic pressure in the solar wind. But the effect of dynamic pressure is very small because the flaring angle of the tail boundary is very small in the distant tail.

After an instantaneous solar wind aberration correction, *Nakamura et al.* [1996] find that all five cases are distributed around the magnetopause boundary (between the two lobe radii of 24 and 29 R_e). In a recent study, *Williams et al.* [1994] find that the magnetosheath encounters are consequences of solar wind aberration effects. However, our study shows that more than 20% of the time the spacecraft locations relative to the tail cannot simply be interpreted by the solar wind (V_x and V_y) aberration effect. *Kokubun et al.* [1996] list 23 large tail (> 20 nT) field events detected by GEOTAIL during magnetic storms. They find that the unusual strongest lobe encounter (53 nT) cannot be explained in terms of solar wind aberration and external pressure, unless the magnetic flux increase does not reduce the tail radius. We find during two intervals of stable northward B_z, the spacecraft is in the magnetosheath, even though its location is very close to the nominal tail axis. The long stable northward IMF may cause disappearing of the distant tail as proposed by *Fairfield [1993]* or a filament tail structure.

Actually, dayside magnetic merging during the southward IMF may cause a magnetic flux increase in the near tail. During the expansion phase of a substorm, the tail flux will decrease due to the near-earth reconnection [*Baker et al.*, 1987]. These changes will not be directly related to the sheath pressure. Thus the changes of tail size cannot be deduced based on the flux conservation under this situation. As in the case we see during the second storm (at -0600 UT, day 36), there is an obvious unbalance between the lobe and the sheath in total pressures, If a reconnection occurs in the distant tail during this time, the tail lobe field flux may not be constant, The tail size will rapidly change to reach a steady state. As a result, we see some plasmasheet crossings which are associated with earthward plasma jetting and slow-mode shocks at 0535 UT or later. Various models have been proposed to explain how the magnetic flux is added and then is cut off during the dayside magnetopause reconnection,

Another reason may be that the magnetic tail is not cylindrical as we assumed in Figure 1. The tail often is twisted or deformed by the IMF B_y effect [*Sibeck et al., 1985*]. We have also detected very large BY (-30 nT) in our three storm events. Thus, the. changes related to IMF variations would also cause multi-crossings when the spacecraft is near the nominal magnetopause. Recent global MHD simulation shows that most magnetosheath encounters may be due to IMF rotations from northward to duskward [*Frank et al.*, 1995], But tail twisting and flattening can only explain transient crossings, near to the magnetopause.

Magnetosheath encounters reported by *Nakamura et al.* [1996] have a time scale of 2- 18 min. while the magnetic tail lobe encounters reported by *Kokubun et al.* [1996] have -20 min duration. In our study we find that most tail lobe encounters have a duration from 10 ruin to 1 hour and the separation between two encounters is 2 - 3 hours, These have been explained due to magnetopause surface waves related to solar wind oscillation [*Sibeck et al.*, 1985]

For those high speed plasma jetting events, because their speed is far higher than the sheath solar wind flow, a reconnection process should occur in the distant tail. However, the question is whether or not these distant neutral lines arc always present (independent of magnetic storms and solar wind) and do they have any relationship with a near-earth neutral line. We suggest that a distant neutral line which is independent of the near-earth neutral line probably always exists. *Ho et al.* [1 994] have reported a near-cornpletc distant reconnection case which includes a pair of slow-mode shocks, bidirectional plasma flows and plasmasheet B_z reversals. Because some such signatures are detected during northward IMFs, *Ho and Tsurutani* [1995] have proposed a model to explain the distant neutral line formation during both northward and southward B_z situations.

These plasma jetting events mainly occur after a magnetic field compression process. It is possible that some external solar wind energies are transferred into the tail though the compression process or other unknown paths (e.g. the opening of the tail) during main phase. After storm these energies store.d inside the plasmasheet arc released as the plasma jetting signatures. Also during recovery phase, both the sheath and tail lobe fields become very low (- S nT, even lower than that before the storm). We expect that there is a tail expansion under such low field strength. 'l'his makes easily for the spacecraft to enter the plasmasheet and to detect these jetting flows. We have seen that the spacecraft goes back and forth between the tail lobe and the plasmasheet boundary layer/plasn]ashect. Bidirectional jetting flows arc detected during two magnetic storms (Storms 2 and 3). For the first storm we do not see any jetting, The spacecraft may not get into ttrc plasma asheet deep enough.

5. Summary

We have examined the ISEE-3 distant tail data during the five strongest magnetic storms (Dst < -100 nT) and identified the tail signatures with high speed solar wind streams, magnetic clouds and near-earth storms. Three of the storm events with obvious distant tail encounters have been studied in detail. We have characterized the field and plasma parameters in the. different tail regions during both storm and quiet times.

1. During the storm onsets, the strong solar wind and magnetic field fluctuations move the tail back and forth across the spacecraft. The lobe field strengths may be predicted under an assumption of the balance between the inside tail lobe magnetic pressure and outside sheath thermal and magnetic pressure,

2. During storms, the distant tail is strongly compressed by the outside sheath pressure. The field magnitudes in the lobe and plasm asheet increase by a factor of 3-5 relative to quiet times. The temperature and density in both regions also increases by a factor of 2-3, while plasma β changes very little, as expected.

3. The strongest magnitude of lobe field we detected during a storm main phase is 37 nT (Jan. 10), which is higher than the sheath field by 5 -10 nT. But three tail lobe encounters, seen also during main phases, show a pressure unbalance between

the lobe (lower field B and plasma density) and the adjacent sheath, It may suggest that the tail is unstable or developing during these intervals,

4. Except for the tail size changes due to field strength changes under an assumption of the tail flux conservation, we also find that the orientation of nominal tail axis is strongly affected by solar wind speed V_y and V_x components. More than 70% of tail crossing events may be predicted by the changes of tail size due to the pressure balance and solar wind directional changes The remaining cases may be caused by the effect of solar wind V_z and flux changes due to reconnection.

S. Nine tail plasmasheet jettings and slow-mode shocks have been detected in the second and third storms. One remarkable feature of the. jettings is very strong earthwai c1 (up to 1200 km/s) and tailward flows (1 500 km/s compared to 900 km/s solar wind speed), and quasi-periodic (- 3 hour) characteristics. The preponderance of such earthward flowing events indicates that during magnetic storms, magnetic reconnection is occurring at locations well beyond the distance of ISEE-3.

6. Through the interface of slow-mode shocks between the tail lobe and the plasmasheet/boundary layer, the magnetic energy is converted into plasma thermal and kinetic energy by the magnetic merging process. The calculated plasma jetting speed (987 km/s) based On a Petschek siow shock model is consistent with observations (1000 km/s) in the boundary layer.

7. Plasmasheet plasma jetting events are mostly detected during the recovery phases of the storms, when the heated plasmasheet expand under a reduced sheath pressure. These plasma jetting events arc probably independent of near-carti] reconnection anti AE index. However, during the storms, because the distant taii is compressed by the high speed solar wind streams, some external energies may be transferred and stored inside the tail through some. unknown mechanisms. As an after-effect, these extra magnetic taii energies is released by field sloughing via the.sc reconnection events.

Acknowledgments: The research conducted at the Jet Propulsion Laboratory, California Institute of Technology was performed under contract to the National Aeronautics and Space Administration.

The Editor thanks two referees for their assistance in evaluating this paper.

References

Baker, D.N, R.C. Anderson, R. D. Zwickl, and J, A, Slavin, Average plasma and magnetic filed variations in the distant magnetotail associated with near-crir[h substorm effects, *J. Geophys. Res.*, 92, 71, 1987.

Bame, S. J., J. R, Asbridge, H. E. Felthauser, J.P. Gore, G. Paschmann, P. Hemmerich, K. Lehman, and H. Rosenbauer, ISEE-1 and ISEE-2 fast plasma experiment and the ISEE-3 solar wind experiment, *IEEE Trans. Geosci. Electron.*. Gl;-16, 216, 1978.

Colburn, D. S., and C. P. Sonnett, Discontinuities in the solar wind, *Space Sci. Rev*,, .5, 439, 1966.

Coroniti, F. V., and C.F. Kennel, Changes in magnetospheric configuration during the substorm growth phase, *J. Geophys.* Ref., 77, 3361, 1972.

Cowley, S. W.H., 'f 'he distant geomagnetic tail in theory and observation, in *Magnetic Reconnection in Space and Laboratory Plasma*, Edited by Hones, E. W.,Jr., AGU, W ashington, DC, *Geophys. Monogr. Ser. 30*, 2.28, 1984.

Fairfield, D.H., Solar wind control of the distant magnetotail: ISEE-3, *J. Geophys. Res.*, 98, 2126S, 1993.

Frandsen, A. M, A., B. V. Connor, J. Van Amersfoort, and E. J. Smith, The ISEE-C vector helium magnetometer, *IEEE Trans. Geosci. Electr. GE-16*, 195, 1978.

Frank, L.A., et al., Observations of plasma and magnetic field in Earth distant magnetic tail: Comparison with a global MHD model, *J. Geophys. Res.*, 100, 19177, 1995.
Hill, 'I'. W., Magnetic merging in a collisionless plasma, *J. Geophys. Res.*, *80*, 4689, 1975.
Ho, C.M., and B.T.Tsurutani, Distant Tail Plasma Jetting and B, Properties at Slow-Mode Shocks: A model of Reconnection During Northward IMFs, *Geophys. Res. Lett.*, 22, 2977, 1995.
no, C. M.. B.T.Tsurutani, E.J. Smith. and W.C.Feldman, A detailed examination of a X-1ine region in the distant tail: ISEE-3 observations of jet flow and B_z reversals and a pair of slow shocks, *Geophys. Res. Lett.*, 21, 3031, 1994.
}1o, C.M., B.T.Tsurutani, E.J.Smith, and W.C.Feldman, Properties of Slow-mode Shocks in the Distant (>200 R_e) Geomagnetic Tail, *J. Geophys. Res.*, 101, 15277, 1996.
Klein, L.W., and L.F.Burlaga, Interplanetary magnetic clouds at 1 AU, *J. Geophys. Res.*, 87, 613, 1982.
Kokubun, S., L.. A. Frank, K. Hayashi, Y. Kamide, R.P. Lepping, '1'. Mukai, R. Nakamura, W.R. Paterson, T. Yamamoto, and K. Yumoto, Large field events in the distant magnetotail during magnetic storms, *J. Geomag. Geoelec.*, 48, 561, 1996.
Nakamura, R., S. Kokubun, Y. Kamide, K. Yumoto, T. Yamamoto, L. A , Frank, W.R. Paterson, E. Frii - Christensen, K. Hayashi, T. Iyemori, H. Luhr, and O.A. Troshichev, Observations of the magnetosheath near the nominal tail axis during the geomagnetic storm of January 25, 1993, *J, Geomag. Geoelec.*, 48, 577, 1996.
Petschek, H.E., Magnetic field annihilation, in AA S-NASA Symposium on the Physics of Solar Flares, edited by W.N.Hess, *NASA Spec. Publ. 50, 425,* 1964.
Saito, Y., '1". Mukai, T.Terasawa, A. Nishida, S. Machida, M.Hirahara, K. Maezawa, S. Kokubun, and T. Yamamoto, Slow-mode shock in the magnetotail, *J. Geophys. Res., 100,* 23567, 1995.
Sibeck, D.G., G.L. Siscoe, J.A. Slavin, E.J. Smith, B.T. Tsurutani, and R. P. Lepping, The distant magnetotail's response to a strong interplanetary magnetic field B_y: twisting, flattening, and field line bending, *J. Geophys. Res.*, 90, 4011, 1985.
Slavin, J. A., E.J. Smith, D.G.Sibeck, D.N. Baker, R.D. Zwickl, and S.-I. Akasofu, An ISEE-3 study of average and substorm conditions in the distant magnetotail, *J. Geophys. Res.*, *90*, 10875, 1985.
Tsurutani, B.T., J.A. Slavin, E.J.Smith, R. Okida, and D.E. Jones, Magnetic structure of (he distant geotail from -60 to -220 R_e: ISEE-3, *Geophys. Res. Lett.*, 11, 1, 1984.
Tsurutani, B.T., B.E. Goldstain, M.E. Burton and D.I . Jones, A review of the ISEE-3 geotail magnetic field results, *Planet. Space Sci.*, .?4, 93 I, 1956.
Tsurutani, B.T., W.D. Gonzalez, F. '1'arm, S,1, Akasofu, and E.J. Smith, Origin of interplanetary southward magnetic fields responsible for major magnetic storms near solar maximum (1978-1979), *J. Geophys. Res.*, 93, 8519, 1988.
Vasyliunas, V, M., Theoretical models of magnetic field line merging, 1, *Rev. Geophys. Space Phys., 13, 303, 1* 97S.
Williams, D.J. et al., Magnetopause encounters in the magnetotail at distances of ~80 R_e, *Geophys. Res. Lett.*, 25, 3007, 1994.
Zwickl, R.D., D.N. Baker, S.J. Bame, W.C. Feldman, J.'1'. Gosling, E.W. Hones Jr., and D.J. McComas, Involution of the Earth's distant magnetotail: ISEE-3 electron plasma rcsu lts, *J. Geophys. Res.*, 89, I 1,007, 1984.

C.M. Ho, and B. T. Tsurutani, MS 169-506, Jet Propulsion Laboratory, California Institute of "1'ethnology, Pasadena, CA 91109 (email: cho@jplsp.jpl.nasa.gov).

(Received May 10, 1996; revised September 15, 1996;
accepted October 25, 1996,)

Paper number 96 JA00545.
0148 -0227 /96/96 JA-00545$09.00

Figurc Captions

Figurc 1. ISEE-3 locations relative to the tail axis during three magnetic storms in Y-Z plane (tail cross-section). The center of the tail has a -15 R_e shift in +Y direction after an aberration (-4°) correction, Tail section is approximately shown as a cylindrical with - 30 R_e radios. Based on this sketch, two cases occur inside the tail, while onc case is seen near the tail boundary, though exact location relative to the tail much depend on solar wind flow rrnd tbc size variations,

Figurc 2. ISEE-3 observations of magnetic field and plasma in the distant tail during magnetic storm on Jan. 9-13,1983. Top two panels give near-earth substorm (AE) and storm (Dst) indices. A large high speed solar wind stream and magnetic cloud last more than two days, Five tail lobe crossings with very strong field strength are identified, Before the storm main phase, large sheath pressure has cause the. increase of lobe field.

Figurc 3. A magnetic storm occurred *on* Aug. 7- 11, 1983 and the distant tail observations. During this period, the solar wind flow speed does not increase much. But magnetic cloud B_z turns southward twice, Wc see many tail lobe crossing and plasma jetting events in the recovery phase.

Figurc 4. A long duration magnetic storm with two main phases and the distant tai] measurements. Solar wind speed increases significantly from -450 to -900 km/s, while the sheath field reach a value as large as - 45 nT. Many tail crossings and plasma jetting are seen during main and recovery phases.

Figurc 5. A detail identification of each distant taii region with high resolution data. Two days of data arc divided into 4 plots: a) pre-storm; b) first storm onset; c) second storm onset and d) early recovery phase. Three regions arc marked out: blank, magnetosheath; hatched, taii lobe and black, plasmashee t.

Figurc 6. AE dependence of the occurrence rates of tail lobe crossings (top) and plasmasheet earthward plasma jettings (bottom). 'There arc relatively more tail lobe crossings when AE index is between 300 and 500 nT, which is mainly attributed to tail lobe staying during late recovery phases of storms 2 anti 3. Earthward jetting events have no dependence on substorm activity. 'There are no obvious changes for different lag times of AE index relative to the tail observations,

Figurc 7. Pressure balance between the sheath and tail lobe and spacecraft relative location to the tail center for three magnetic storms. Solid line give the distance of spacecraft relative to a solar wind aberration corrected tail axis, Dashed line give the tail size which varies depending on predicted tail field strength under an assumption of tail flux cons, creation, Dotted line is the distance from a tail center which just corrected by a fixed aberration (4°) angle. A relative variation of the solid iine to the dashed line will show how spacecraft gets in and out from the tail.

Figurc 8. A strong plasma jetting and slow-mode shock event detected around 2000 UT, Feb. 5, 1983. Magnetic field aiso is rotate.d into a shock frame (B_i, B_j and B_k). Earthward plasma flow is detected in the region of plasmasheet boundary layer. We have identified' the interface between the lobe and plasmasheet as a slow-mode shock using coplanar theorem and R-ii relation.

Figurc 9. A sketch to show the geometry of slow-mode shock anti plasma jetting location. The spacecraft entry from anti exit into the south lobe across the slow-mode shock and boundary layer earthward the neutral line. Ail shock parameters arc calculated anti compared with the real measurements.

Figurc 1. ISEE-3 locations relative to the tail axis during three magnetic storms in Y-Z plane (tail cross-section). The center of the taii has a ~15 R_e shift in +Y direction after an aberration (-4°) correction, Tail section is approximately show, n as a cylindrical with - 30 R_e radius. Based on this sketch, two cases occur inside the tail, while onc case is seen near the tail boundary, though exact location relative to the tail much depend on solar wind flow and the size variations,

Figurc 2, ISEE-3 observations of magnetic field and plasma in the distant taii during magnetic storm on Jan, 9 - 13,1983. Top two panels give near-earth substorm (AE) and storm (Dst) indices. A large high speed solar wind stream and magnetic cloud last more than two days, Five tail lobe crossings with very strong field strength are identified. Before the storm main phase, large sheath pressure has cause the increase of lobe field,

Figurc 3. A magnetic storm occurred on Aug. 7- 1i, 1983 and the distant tail observations, During this period, the solar wind flow speed dots not increase much. But magnetic cloud B_z turns southward twice. Wc see many tail iobc crossing and plasma jetting events in [he. recovery phase.

Figure 4. A long duration magnetic storm with two main phases and the distant tail measurements. Solar wind speed increases significantly from -450 to -900 km/s, while the sheath field reach a value as large as - 45 nT. Many tail crossings and plasma jetting are seen during main and recovery phases.

Figure 5. A detail identification of each distant tail region with high resolution data. Two days of data are divided into 4 plots: a) pre-storm; b) first storm onset; c) second storm onset and d) early recovery phase. Three regions are. marked out: blank, magnetosheath; hatched, tail lobe and black, plasmasheet.

Figure 6. AE dependence of the occurrence rates of tail lobe crossings (top) and plasmasheet earthward plasma jettings (bottom). "There are relatively more tail lobe crossings when AE index is between 300 and 500 nT, which is mainly attributed to tail lobe staying during late recovery phases of storm 2 and 3. Earthward jetting events have no dependence on substorm activity. There are no obvious changes for different lag times of AE index relative to the tail observations.

Figure 7. Pressure balance between the sheath and tail lobe and spacecraft relative location to the tail center for three magnetic storms, Solid line give the distance of spacecraft relative to a solar wind aberration corrected tail axis. Dashed line. give the tail size which varies depending on predicted tail field strength under an assumption of tail flux conservation Dotted line is the distance from a tail center which just corrected by a fixed aberration (4°) angle. A relative variaticm of the solid line to the dashed line will show how spacecraft gets in and out from the. tail.

Figure 8. A strong plasma jetting and slow- mode shock event detected around 2000 UT, Feb. 5, 1983. Magnetic field also is rotated into a shock frame (B_i, B_j and B_k). Earth ward plasma flow is detected in the region of plasmasheet boundary layer. We have identified the interface between the lobe and plasmasheet as a slow- mode shock using coplanar theorem and R-H relation.

Figure 9. A sketch to show the geometry of slow- mode shock and plasma jetting location. The spacecraft entry from and exit into the sooth lobe across the slow-mode shock and boundary layer earthward the neutral line. All shock parameters are calculated and compared with the real measurements.

Table 1. Three Magnetic Storm Data Interval, Dst and ISEE-3 Trajectory Coverages

Storm Events	Data Intervals	Maximum Dst	Trajectory Ranges
Case 1	Day 009-013, 1983	-220 nT	$-166.8 > X > -181.5\ R_e$
Case 2	Day 034-042, 1983	-185 nT	$-219.5 > X > -219.9\ R_e$
Case 3	Day 219-223, 1983	-150 nT	$-221.6 > X > -217.9\ R_e$

Table 2. Distant Tail Parameters During Storm and Quiet Times

Time	Regions	|B| nT		N_e cm^{-3}		T_e K		V km/s		β rate	
		storm	quite	storm	quiet	storm	uiet	storm	quiet	storm	quiet
Jan. 9	M'sheath	27	10	22	5	3.3×10^5	1.5×10^5	600	450	0.31	0.26
-13,	Tail Lobe	37	8	1.0	0.55	8.0×10^5	4.0×10^5	250	150	0.02	0.11
1983	P'sheet	8	3	0.5	0.22	1.3×10^6	1.0×10^6	750	500	0.35	0.77
Feb. 3	M'sheath	45	7	40	8	0.6×10^5	0.2×10^5	900	500	0.43	0.35
-10,	Tail Lobe	28	12	0.2	0.05	1.0×10^6	0.7×10^6	600	300	0.01	0.01
1983	P'sheet	5	2	0.6	0.1	3.5×10^6	1.5×10^6	1300	800	2.9	1.3
Aug.7	M'sheath	25	10	20	6	2.0×10^5	1.0×10^5	500	400	0.22	0.20
-11,	Tail Lobe	31	14	2	0.5	6.0×10^5	5.0×10^5	200	150	0.04	0.04
1983	P'sheet	8	2	0.2	0.1	1.5×10^6	1.0×10^6	1000	800	0.16	0.87

Table 3. Plasma Jetting and Slow-mode Slow Parameters

B_u (nT)			B_d (nT)			B_n (nT)		V_u (km/s)		V_d (km/s)		Shock Normal $\boldsymbol{n}$		
-8.30,-0.03,-0.54			-0.26,-4.24,-5.3			-5.23		210		940		-0.38,0.27,0.89		
N_u	N_d	T_u	T_d	θ_{Bnu}	θ_{Bnd}	θ_{nz}	ξ	η	V_{Au}	V_{Aun}	V_{nu}	V_{sl}	M_{An}	β
0.22	0.04	1.5×10^6	$.0\times10^6$	71.5	38.8	27.6	21.2	70.6	1300	862	576	243	0.68	0.05

ISEE 3 Locations Relative to the Tail Axis During Three Magnetic Storms

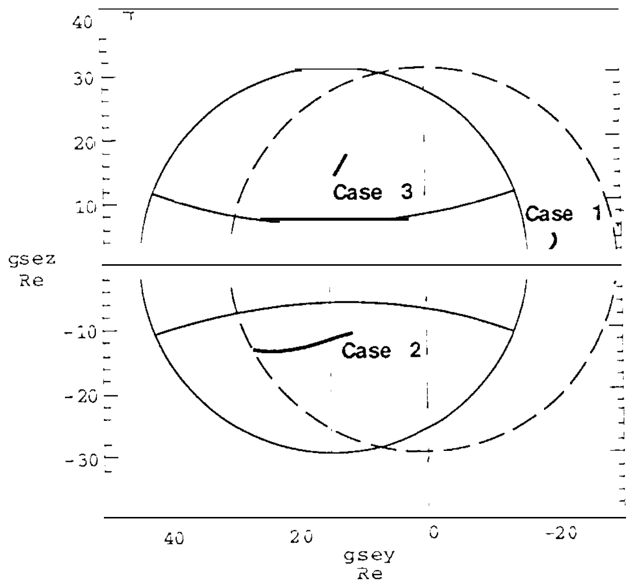

Fig. 1

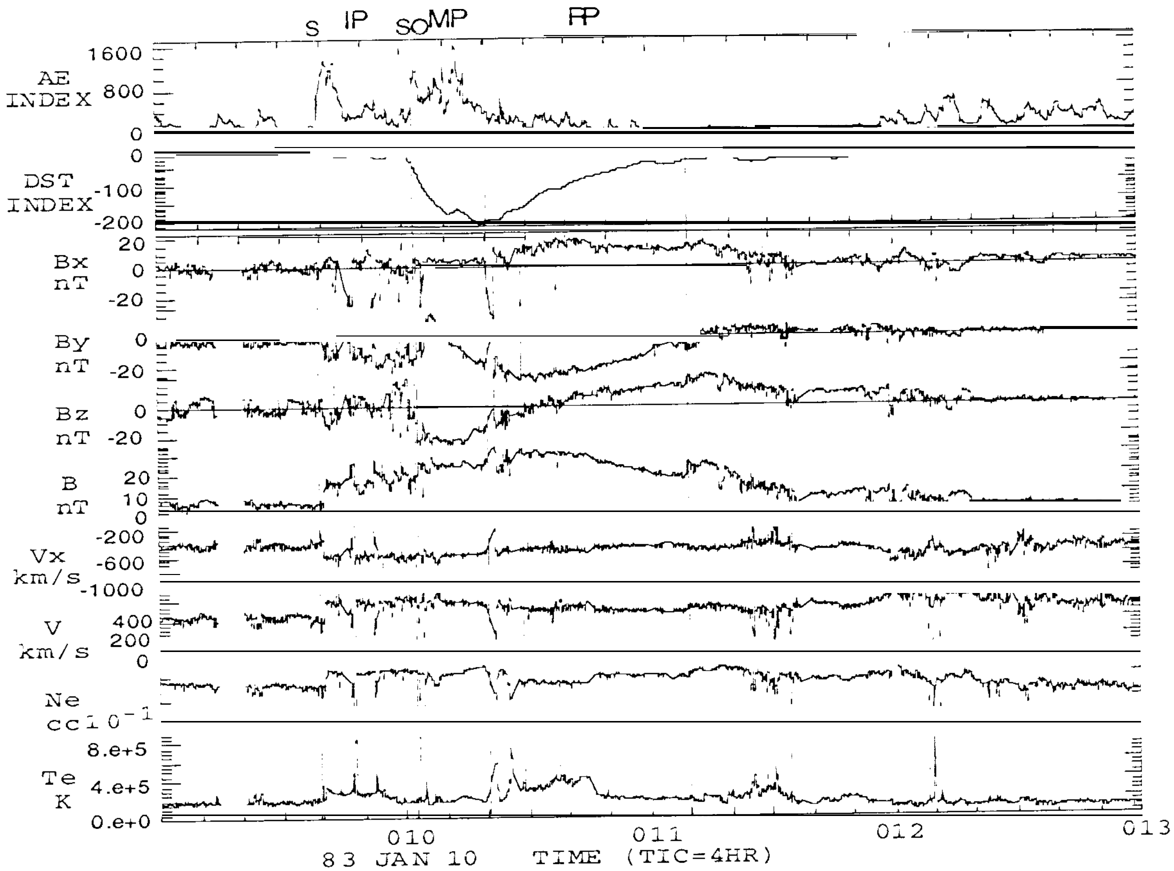
S
IP
SO
MP
FP
AE INDEX
1600
800
0
DST INDEX
0
-100
-200
Bx nT
20
0
-20
By nT
0
-20
Bz nT
0
-20
B nT
20
10
0
Vx km/s
-200
-600
-1000
V km/s
400
200
0
Ne $cc10^{-1}$
Te K
8.e+5
4.e+5
0.e+0
010
011
012
013
83 JAN 10 TIME (TIC=4HR)

Fig. 2

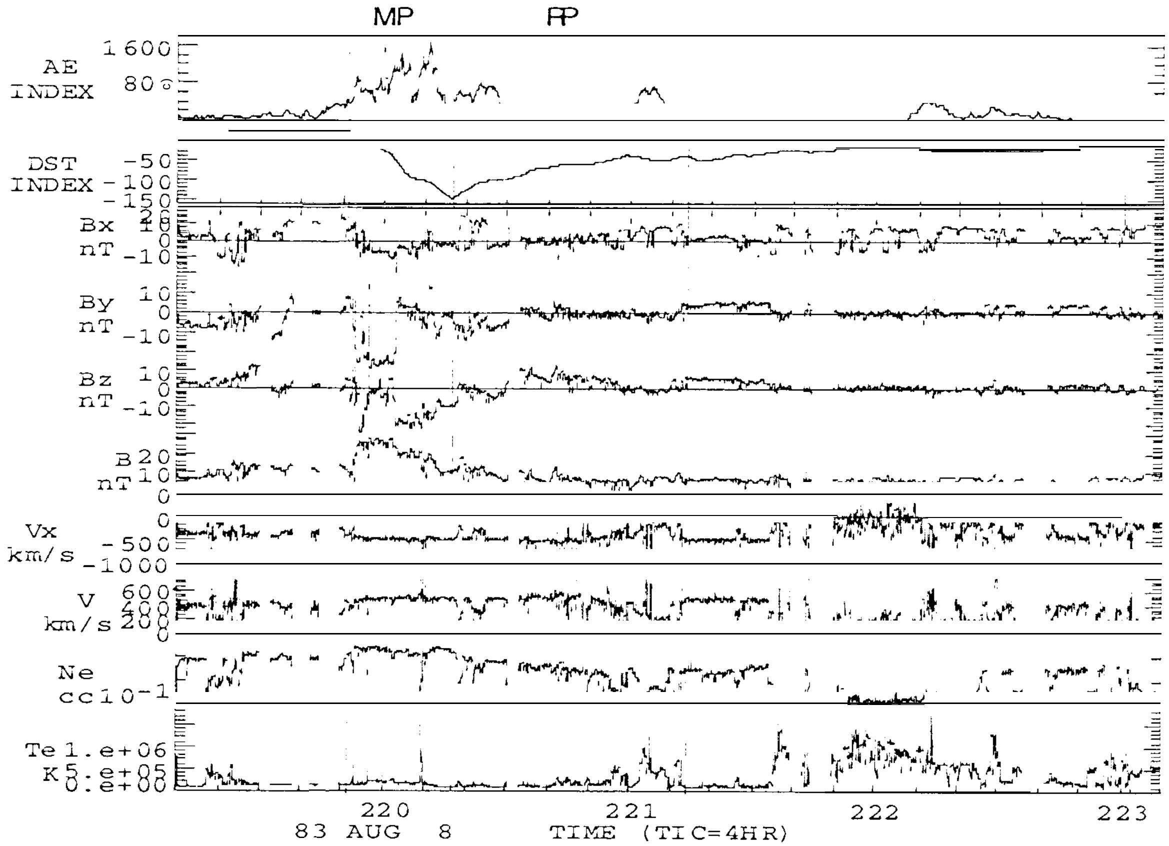
MP
FP
AE INDEX
1600
800
DST INDEX
-50
-100
-150
Bx nT
By nT
Bz nT
B nT
Vx km/s
V km/s
Ne cc10-1
Te K
220
221
222
223
83 AUG 8
TIME (TIC=4HR)

Fig 3

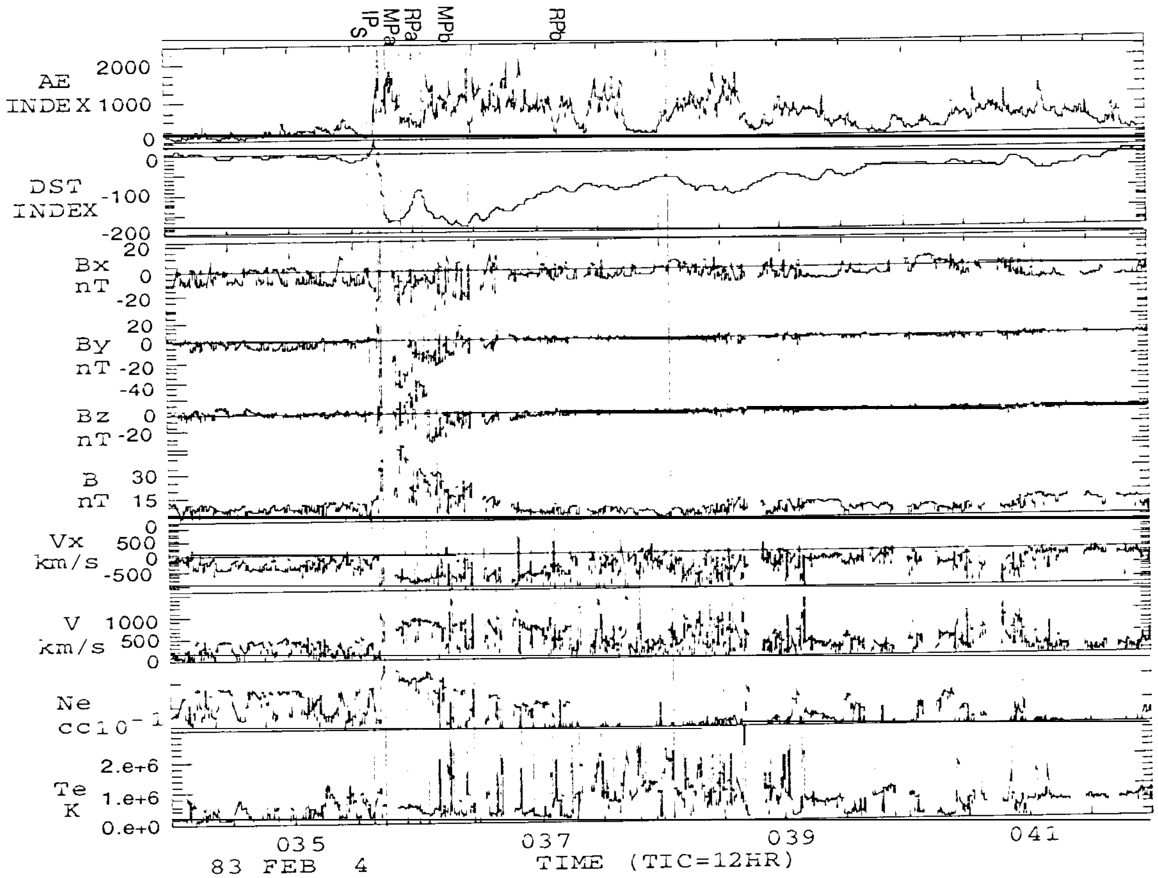

IPS
MPa
RPa
MPb
RPb
AE INDEX
2000
1000
0
DST INDEX
0
-100
-200
Bx nT
20
0
-20
By nT
20
0
-20
-40
Bz nT
0
-20
B nT
30
15
0
Vx km/s
500
0
-500
V km/s
1000
500
0
Ne cc10⁻¹
Te K
2.e+6
1.e+6
0.e+0
035
037
039
041
83 FEB 4
TIME (TIC=12HR)

Fig. 4

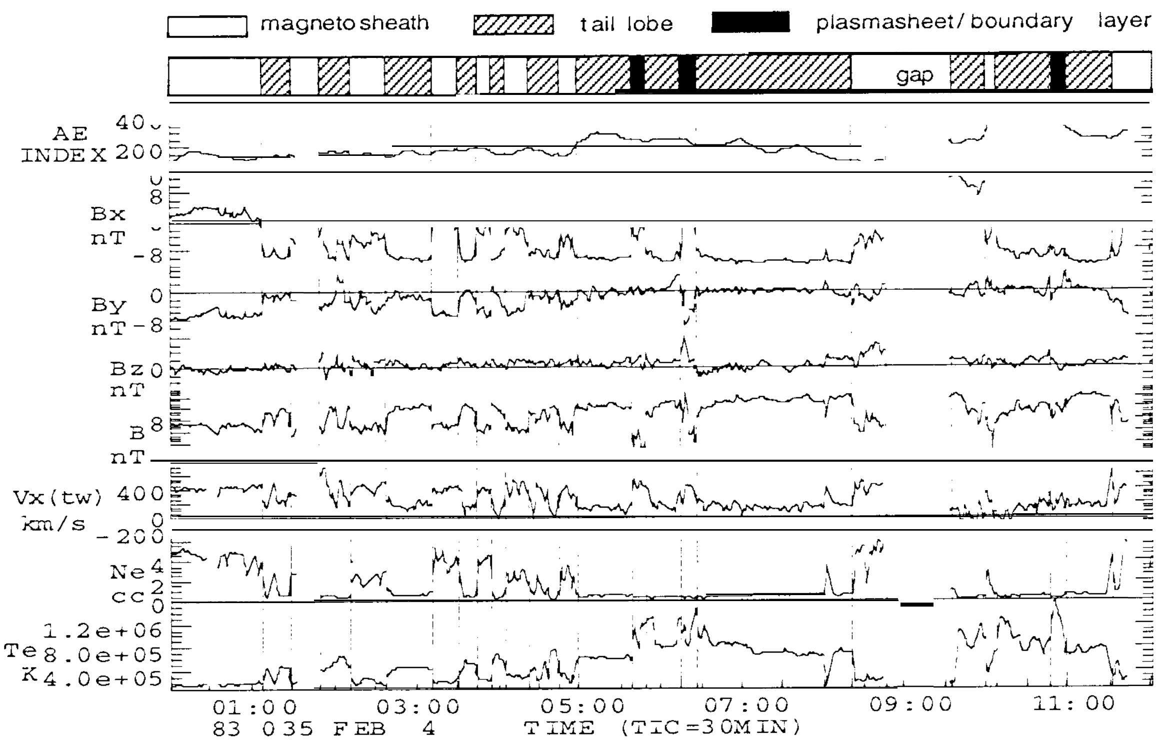

magnetosheath
tail lobe
plasmasheet/boundary layer
gap
AE INDEX
Bx nT
By nT
Bz nT
B nT
Vx(tw) km/s
Ne cc
Te K
01:00
03:00
05:00
07:00
09:00
11:00
83 035 FEB 4
TIME (TIC=30MIN)

Fig 5a

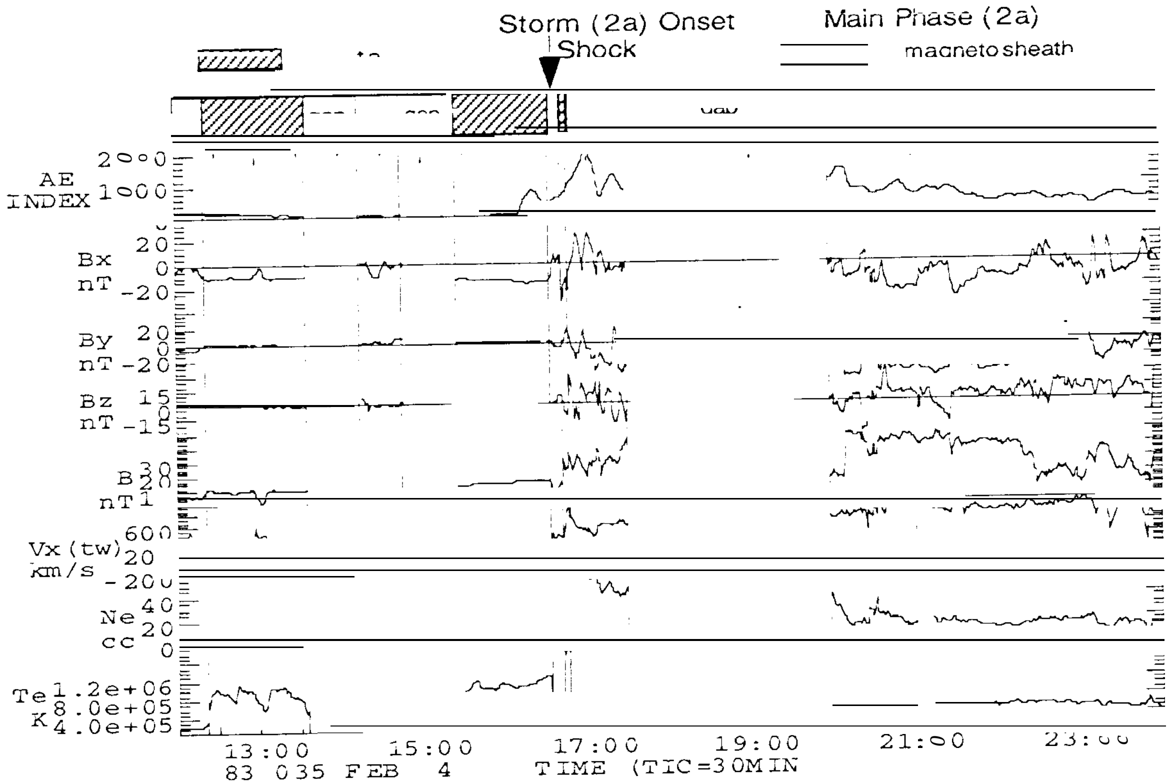
Storm (2a) Onset
Shock
Main Phase (2a)
magnetosheath
AE INDEX
2000
1000
Bx nT
20
0
-20
By nT
20
0
-20
Bz nT
15
0
-15
B nT
30
20
1
Vx (tw) km/s
600
20
-200
Ne cc
40
20
0
Te K
1.2e+06
8.0e+05
4.0e+05
13:00
15:00
17:00
19:00
21:00
83 035 FEB 4
TIME (TIC=30MIN

Fig 5b

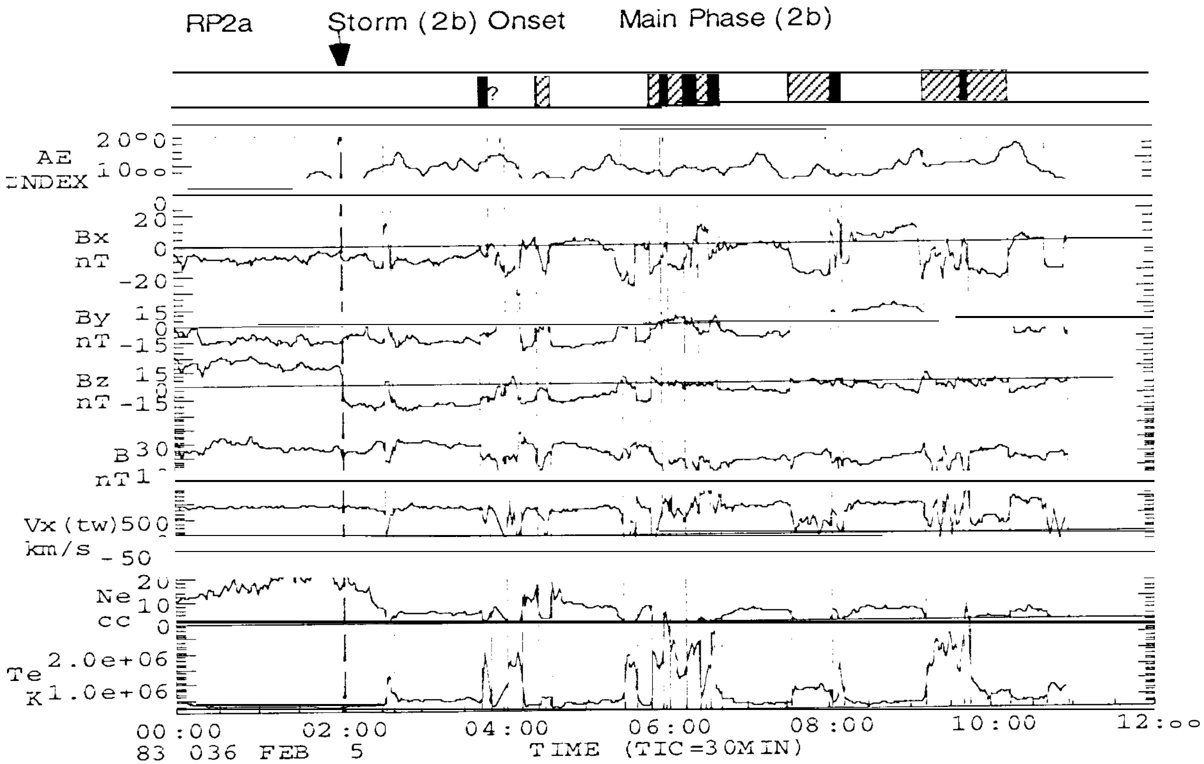
RP2a
Storm (2b) Onset
Main Phase (2b)
?
AE
INDEX
2000
1000
Bx
nT
20
0
-20
By
nT
15
0
-15
Bz
nT
15
0
-15
B
nT
30
Vx (tw)
km/s
500
-50
Ne
cc
20
10
0
Te
K
2.0e+06
1.0e+06
00:00
02:00
04:00
06:00
08:00
10:00
12:00
83 036 FEB 5
TIME (TIC=30MIN)

Fig. 5c

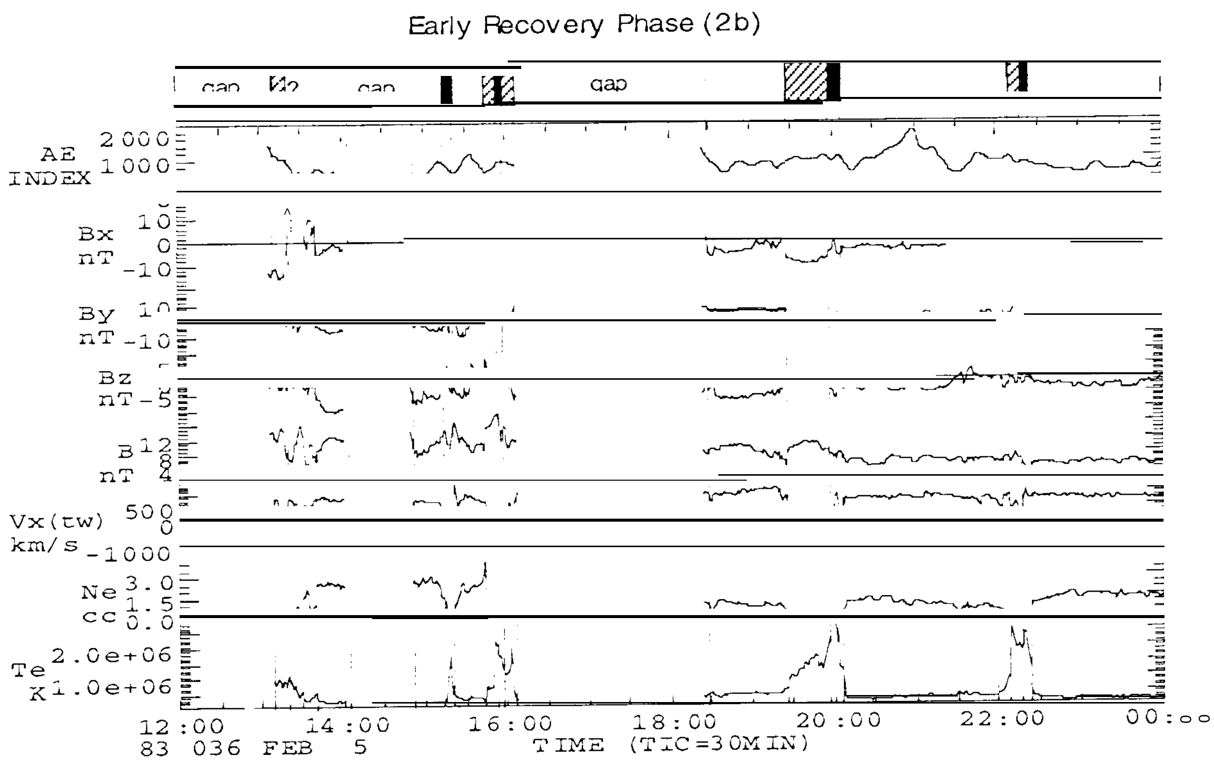
Early Recovery Phase (2b)
gap
gap
gap
AE INDEX
2000
1000
Bx nT
10
0
-10
By nT
-10
Bz nT
-5
B nT
12
8
4
Vx(tw) km/s
500
0
-1000
Ne cc
3.0
1.5
0.0
Te K
2.0e+06
1.0e+06
12:00
14:00
16:00
18:00
20:00
22:00
00:00
83 036 FEB 5
TIME (TIC=30MIN)

Fig. 5c

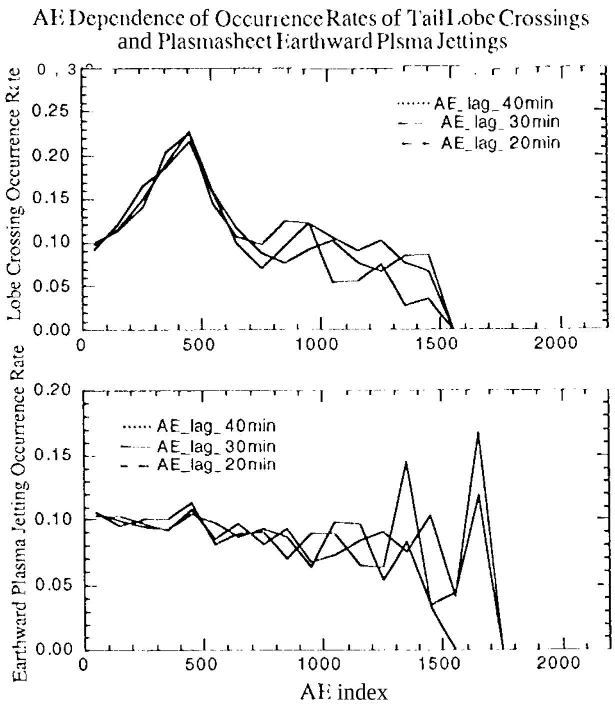
AE Dependence of Occurrence Rates of Tail Lobe Crossings
and Plasmasheet Earthward Plsma Jettings
Lobe Crossing Occurrence Rate
0.25
0.20
0.15
0.10
0.05
0.00
AE_lag_40min
AE_lag_30min
AE_lag_20min
0
500
1000
1500
2000
Earthward Plasma Jetting Occurrence Rate
0.20
0.15
0.10
0.05
0.00
AE_lag_40min
AE_lag_30min
AE_lag_20min
0
500
1000
1500
2000
AE index

Fig. 6

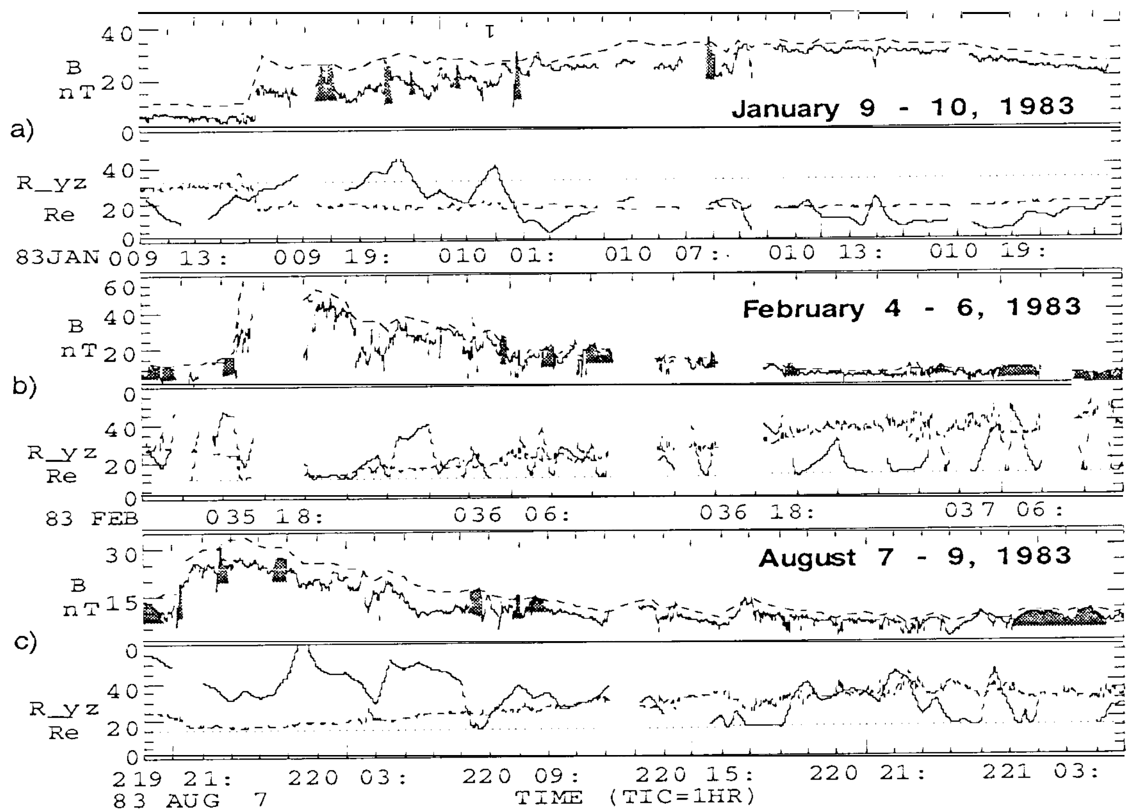

a)
B
nT
R_yz
Re
January 9 - 10, 1983
83JAN 009 13:
009 19:
010 01:
010 07:
010 13:
010 19:
b)
February 4 - 6, 1983
83 FEB
035 18:
036 06:
036 18:
037 06:
c)
August 7 - 9, 1983
219 21:
220 03:
220 09:
220 15:
220 21:
221 03:
83 AUG 7
TIME (TIC=1HR)

Fig. 7

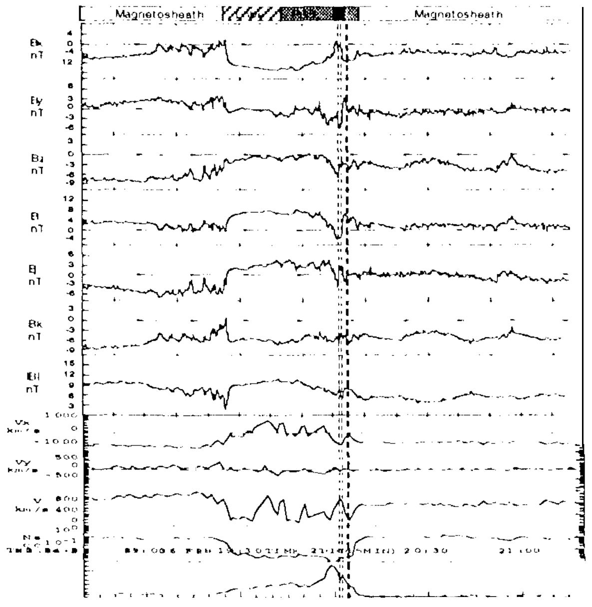

Fig. **8**

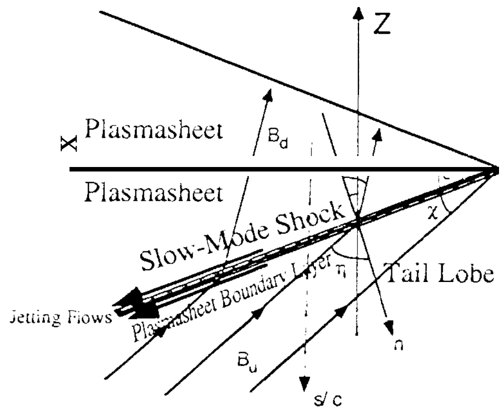
Z
X
Plasmasheet
Plasmasheet
Slow-Mode Shock
Plasmasheet Boundary Layer
Jetting Flows
Tail Lobe

Fig 9